Regular Article

ANALYTICAL AND BIOANALYTICAL CHEMISTRY RESEARCH

Published by the Iranian Chemical Society

Anal. Bioanal. Chem. Res., Vol. 6, No. 2, 271-287, December 2019.

Statistical Optimization of Removal of Safranin Dye from Aqueous System Using Biosorbent Obtained from Leaves of Phlomis Cancellata Bunge by Response Surface Methodology

Somayeh Heydari[a,*], Mohadeseh Hosseinpour Zaryabi[b] and Hamideh Ghiassi[a]

[a]*Department of Chemistry, University of Torbat-e jam, Torbat-e Jam, Iran*

[b]*Department of Chemistry, University of Birjand, Birjand, Iran*

(Received 28 August 2018 Accepted 25 December 2018)

The biosorption performance of Phlomis cancellata Bunge as inexpensive, abundant and easily available adsorbent for safranin cationic dye removal from aqueous system has been evaluated in a batch process, using response surface methodology and employing a central composite design Experimental. The influence of different parameters such as, pH, contact time, agitation rate and sorbent dosage on the removal of safranin was examined. The significance of independent variables and their interactions were tested by analysis of variance (ANOVA). The optimum contact time, pH, agitation speed and adsorbent dose were found to be 39.96 min, 9.0, 331.18 rpm and 20 mg ml^{-1}, respectively. Under these conditions, the maximum sorption capacity for safranin was found to be 99.60%. The kinetics of dye sorption fitted well with pseudo-first order kinetic model. The isotherm data of safranin could be well described by Langmuir model (R^2 = 0.9924). The method was successfully applied for the removal of safranin from industrial wastewater and groundwater samples.

Keywords: Safranin, Removal, Aqueous system, Phlomis cancellata bunge, Response surface methodology

INTRODUCTION

Wastewaters containing hazardous inorganic (metals) or organic (microbes, dyes/pigments) species are considered to be a serious environmental problem in human society. Dyes represent a contaminant of concern for water resources, because of their poor biodegradability and their high diffusion in aquatic environment [1]. They are used as an essential raw material in different industries such as food, paper, plastics, cosmetics and textile [2].

Safranin (3,7-dimethyl-10-phenylphenazin-10-ium-2,8-diamine chloride) is a cationic, azine dye, which is amongst the oldest known synthetic dyes (Fig. 1). Safranin is a water-soluble organic dye, which is mainly used in textile industries [3]. It is also used as food dye in flavoring and coloring candies and cookies and as a biological stain and redox indicator. However, Contact with safranin dye causes several acute effects on health like cornea and conjunctiva in human and rabbit eyes and also skin and respiratory tract irritation [4]. So the removal of dye safranin from the various matrices such as aqueous systems is highly significant.

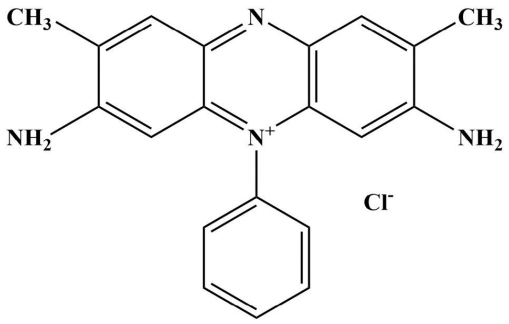

Fig. 1. Chemical structure of safranin.

Various techniques have been applied for the removal of

*Corresponding author. E-mail: so_heydari_83@yahoo.com

dye from wastewater like adsorption [5], coagulation [6], fenton process [7], ozonation [8], chemical oxidation [9], ultrasonic irradiation [10] and membrane process [11]. Among the above techniques, the adsorption of dye molecules onto a substrate (adsorbent) by physical or chemical interactions is arguably one of the most popular methods due to simplicity, convenience, high removal efficiency and low costs [12-14]. Recently, biosorptives have been recognized to have a potential to be a superior adsorbent in the adsorption of dye from wastewater with regard to ease of operation, cost economics, ecocompatibility, high efficiency, simplicity of design, and insensitivity to toxic substances [15]. A considerable number of low-cost biosorbents have been recently applied for removal of dyes from aqueous solutions and raw wastewaters [16]. Khatod evaluated adsorption of dye solution methylene blue using low cost adsorbent like neem leaf and orange peel powder [17]. In this work, a maximum removal of 90-95% was obtained for an adsorbent dose of 0.3 g at 2.5 × 10^{-5} mg ml^{-1} dye concentration. The biosorption performance of raw cone shell of Calabrian pine for C.I. Basic Red 46 as a model azo dye from aqueous system was proposed by Deniz [18].The optimization study revealed that the pine cone shell can be an effective and economically feasible biosorbent for the removal of dye. Lin *et al.* demonstrated that the polyethersulfone/plant-wasteparticles mixed matrix membranes had good pore properties and high ion-exchange capacity so that they could efficiently remove the cationic dyes from water [19]. In this study, three kinds of plant wastes, including banana peel, tea waste, and shaddock peel, were adopted as fillers to fabricate the mixed matrix membranes via water-vapor-induced phase inversion. The performance of lignocel-lulosic residues, pineapple plant stem (PPS) for cationic (Basic Blue 3, BB3) and anionic (Congo Red, CR) dyes removal was evaluated in a batch process, by Chan *et al.* [20]. The result suggested that PPS has higher affinity on cationic than anionic dye. The promising regeneration capability of PPS using acid, implied PPS was a potential biosorbent for BB3 removal.

Phlomis genus belongs to Labiatae (Lamiaceae) family with 70 annual and perennial species which disperse in the world, mostly in Asia [21-23]. Southern and eastern Anatolia and northwestern Iran are presented as the centers of Phlomis species diversity. Representatives of the genus grow as shrubs or subshrub plants with the sessile flowers organized in axillary verticillasters. Some species of *Phlomis* genus are used in folk medicine as a stimulant or tonic and for wound healing, and many studies have shown various biological properties, including anti-inflammatory, immunosuppressive, antimicrobial and antimutagenic activities [24,25]. Phlomis cancellata Bunge that has been known as Gushbarre Irani is aperennial and annual species which can be used more in modern medicine and different industries. Hexadecanoic acid, germacrene D, eudesmol, octacosane, (*E*)-caryophyllene, heptacosane and pentacosane were major components in Phlomis cancellata oil. This plant that grows naturally is very cheap, renewable, and of great availability. Therefore, it is potential lingo-cellulosic biomaterial for dye biosorption. New usage as biosorbent of Phlomis cancellata Bunge is an attractive alternative from both environmental and economic aspects.

Conventional and classical methods of studying a process, to ensure a maximum yield, minimum time, energy and materials consumption in biochemical reactions, by maintaining other factors involved at an unspecified constant level does not depict the combined effect of all the factors involved. These methods are also time consuming and requires a number of experiments to select the best conditions, which are unreliable [26]. Therefore, the design of experiment methods which are based on the multivariate static techniques are appropriate replacements for classical methods to optimize the effective factors on procedures and are more precise in estimating the effect of each factor and are also estimate the interaction between factors [27]. One of the efficient statistical techniques which is used excessively in optimization procedures is response surface methodology (RSM). RSM is a collection of statistical procedures, including selection of the proper experimental design, prediction and verification of various polynomial models, generation of contour plots and 3D response surfaces, and finally determination of optimum values for the factors that employed to maximize the response criteria used [28,29].

The main objective of this study is to optimize the biosorption performance of Phlomis cancellata Bunge leaf for Safranin dye from aqueous system using RSM and employing a central composite design Experimental. The

isotherm models of Freundlich, Langmuir and Dubinin-Radushkevich, were used for the equilibrium data analysis. The kinetic data were analyzed using the pseudo-first-order, and pseudo-second-order models.

EXPERIMENTAL

Biosorbent Preparation and Characterisation

Leaves of Phlomis cancellata Bunge were collected from bakharz region of Khorasan state of Iran in month of April in the year 2017. To remove debris and other contaminated organic contents, leaves of Phlomis cancellata Bunge were washed with deionized water and dried at room temperature. The dried samples were powdered using a sterilized blade and stored until further analysis.

Fourier Transformed Infrared (FTIR) spectrum of Phlomis cancellata Bunge extract within the range of 400-4000 cm^{-1} was recorded on Perkin Elmer 1750 FTIR Spectrophotometer. FT-IR analysis was performed, in order to determine the functional groups on Phlomis cancellata Bunge leaves extract and predict their role in the biosorption of safranin dye. Besides, a Scanning Electron Microscope (SEM) (SEM, TESCAN Mira3) with accelerating voltage of 15 Kv was utilized to disclose the surface morphology of the biosorbent. SEM provides detailed high resolution images of the sample by rastering a focused electron beam across the surface and detecting secondary or back scattered electron signal. Elements presented with samples identified by energy dispersive X-ray spectroscopy (EDX) characterization. The solid addition method was used to determine the point zero charge (pH_{pzc}) of the biosorbent. pH_{pzc} is an important parameter to analyze the surface charge properties of biosorbent. 50 ml of a 0.01 M NaCl solution with pH varying from 2 to 11 and each solution was adjusted by adding 0.10 M of hydrochloric acid or sodium hydroxide. The initial pH of the solution was accurately measured. 0.03 g of the biosorbent was added and the suspension were shaken at 200 rpm for 24 h. The pH values of the supernatant were measured and plotted against the initial pH. The pH_{pzc} of biosorbent was corresponded to the point of intersection when $\Delta pH = 0$.

Sorbate Preparation

Safranin dye (MW = 350.85) were bought from merck and used without further purification. A stock dye solution at a concentration of 100 mg l^{-1} was prepared by dissolving appropriate amount of the dye in distilled water. The experimental concentrations were freshly prepared by the dilution of this solution. The pH values of working solutions were adjusted by the addition of 0.1 M HCl and 0.1 M NaOH solutions whenever necessary.

Batch Dye Adsorption Experiments

Batch studies was carried by weighting 0.02 g biosorbent and added into 10 ml beaker. After 3 ml of dye solution with different concentrations was added into sorbent-containing beaker, the mixture was agitated using rotary shaker. The whole batch studies were carried out at ambient temperature (25 ± 2 °C). Besides, sample without sorbent was served as a control throughout the experiments to ensure the sorption process was performed solely by the sorbent not the inner surface of beaker. Phase separation between dye-adsorbed biosorbent and remaining dye solution was performed naturally within 5 min by gravity. The liquid phase was extracted and proceeded to optical density measurement with a double-beam spectrophotometer (Photonix Ar 2017, UV-Vis Array) with 1 nm resolution and optical length of 1 cm at respective maximum wavelength at λ_{max} (534 nm). Figure 2 shows the zero order absorption spectra of safranin in the wavelength region of 300-600 nm.

The adsorption was calculated using the following formula:

$$q_e = \frac{(C_o - C_e)V}{W} \quad (1)$$

Where, q_e (mg g^{-1}) is the equilibrium adsorption capacity, C_e is the safranin concentration at equilibrium (mg l^{-1}), V is the volume of adsorbate (l) and w is the weight of adsorbent (g).

Experimental Design

Response surface methodology is a kind of experimental design methods. A collection of mathematical and statistical techniques helpful for the modeling and analysis of problems in which a response of favorite is influenced by several variables and the objective is to optimize this response is defined as response surface methodology, or RSM. The main idea of RSM is to use a sequence of

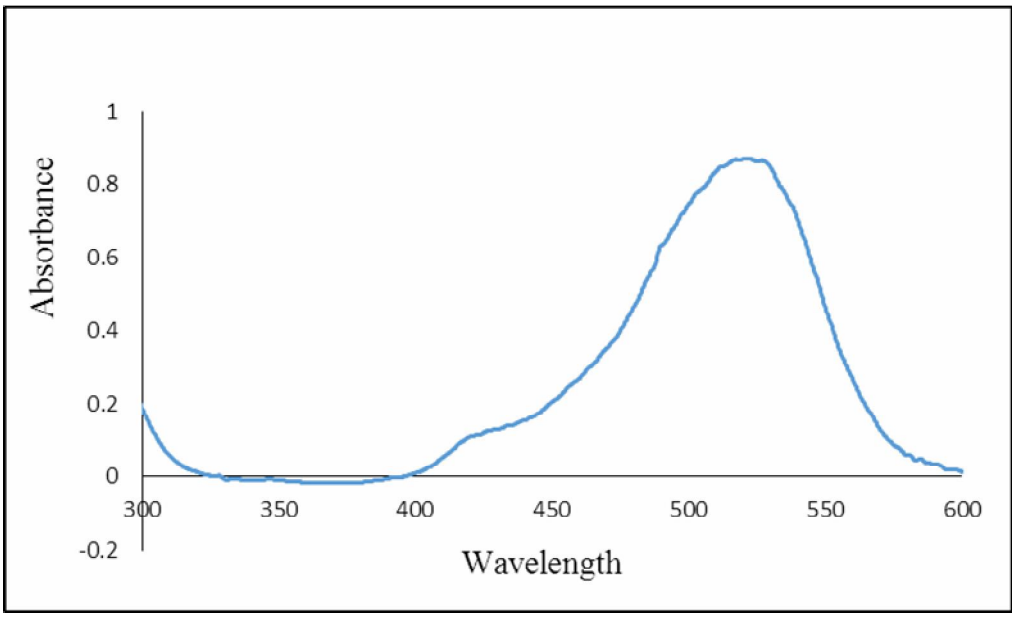

Fig. 2. The zero order absorption spectra of safranin.

Table 1. The Levels Employed for the Different Factors Employed by Experimental Investigations

Name	-α	-1	0	+1	+α
A: pH	3	5	7	9	11
B: Contact time (min)	2.5	15	27.5	40	52.5
C: Agitation speed (rpm)	100	200	300	400	500
D: Adsorbent dose (mg ml^{-1})	10	20	30	40	50

designed experiments to obtain an optimal response. If the fitted surface is a sufficient approximation of the true response function, then analysis of the fitted surface will be nearly equivalent to analysis of the real system.

Central composite design. Central composite design represents a good choice among the standard designs used in RSM, because of its high efficiency with respect to the number of required runs. CCD is to augment a full factorial design by adding so-called star points (set points) and some number of replicate measurements at the center (center points). By spacing all the points at an equal distance from the center, a rotatable design is obtained that gives each point equal leverage in the estimation of the regression coefficients. So, the number of experiments decreases. In this study, the effect of four factors, pH level, Contact Time, Agitation Speed and Adsorbent Dose, on the adsorption of safranin dye on the biosorbent was investigated. The investigated factors and their domains are presented in Table 1. Equation (2) was used to depict the relationship between the coded and real values.

$$X_i = x_i - x_0/\Delta x \quad (2)$$

Where x_i is the dimensionless coded value of i independent variable, X_i is the real value of the independent variable, X_0 is the value of X_i at the center point and ΔX is the step change value.

Utilizing RSM, a quadratic polynomial condition (Eq. (3)) was created for the pre-lingual authority of reaction as a component of autonomous factors and their associations by means of least squares calculation.

$$Y = b_0 + \sum_{i=1}^{n} b_i X_i + \sum_{\substack{i=1 \\ j>i}}^{n-1} \sum_{j=2}^{n} b_{ij} X_i X_j + \sum_{i=1}^{n} b_{ii} X_i^2 \quad (3)$$

Where Y is the response variable to be modelled, X_i and X_j represent the independent variables in the form of coded values, b_0 is the constant coefficient, b_i is the coefficient of linear effect, b_{ij} is the coefficient of interaction effect, b_{ii} the coefficients of quadratic effect and n is the number of variables.

The experiments were performed in three blocks of 36 sets of test conditions at five levels with one replicate and operated in a randomized arrangement to avoid systematic bias. The data analysis is carried out for each response variable described in the following sections as shown in Table 2. The analysis of results was performed with statistical and graphical analysis software (Design Expert, Version 7.1.5 Trial). Design Expert software was used for regression analysis of the data obtained and to estimate regression equation coefficient.

Figure 8 shows 3D response surfaces and contour plots of the model. The responses were mapped against two experimental factors while the other factors are held constant at its central level. The adequacy of each model was checked using the F-values, lack of fit, and R^2-values, and finally a quadratic model was adopted. The statistical significance of the full quadratic models predicted was considered by the analysis of variance (ANOVA). The ANOVA results of the quadratic model are summarized in Table 3.

Isothermal Modeling

In order to understand the mechanism of adsorption process, isothermal studies are carried out for the complex binary dye solution. Two isotherms namely Langmuir and Freundlich isotherms are applied and presented as Eqs. (4) and (5), respectively.

$$C_e/q_e = 1/bq_m + C_e/q_m \quad (4)$$

$$q_e = K_f C_e^{1/n} \quad (5)$$

Where q_m is the maximal monolayer adsorption extent of the used adsorbent, b is the Langmuir adsorption constant. Whereas, K_f and 1/n are the constant factors dealing with adsorption capacity and intensity respectively. Langmuir model explains monolayer adsorption, while Freundlich directs towards heterogeneous adsorption indicating a multilayer sorption. The details of all the isotherm models are given in Table 4.

Dubinin-Radushkevich model is generally used to express the nature of adsorption as physically and chemical [30] and can be presented as Eq. (6).

$$\ln q_e = \ln(q_m) - K\varepsilon^2$$

Where q_e is the amount of dye adsorbed at the equilibrium, k is a constant related to the adsorption energy, q_m is the theoretical saturation capacity, and ε is the Polanyi potential which is equal to

$$\varepsilon = RT \ln(1 + 1/C_e) \quad (6)$$

In Dubinin-Radushkevich isotherm, the mean free energy, E (kJ mol^{-1}), shows the mechanism which sorption takes place (*) and defined by Eq. (7)

$$E = 1/\sqrt{2\varepsilon} \quad (7)$$

A value of mean free energy below 8 kJ mol^{-1} displays physical biosorption while a value between 8 and 16 kJ mol^{-1} indicates chemical biosorption.

Adsorption kinetics investigation provides an idea for understanding the adsorption mechanism. Adsorption kinetic based on pseudo-first-order model represented by Eq. (8) [31].

Table 2. Actual Values of the Independent Variables Set and Corresponding Values of the Response Variables for Safranin

Run	Block	Factor1 A: pH	Factor 2 B: Contact time (min)	Factor 3 C: Agitation speed (rpm)	Factor 4 D: Adsorbent dose (mg ml^{-1})	Response %Removal
1	Block 1	7	27.5	300	30	60.08
2	Block 1	5	15	400	20	52.00
3	Block 1	9	15	400	40	56.23
4	Block 1	5	40	200	20	88.59
5	Block 1	5	40	400	40	81.77
6	Block 1	9	40	200	40	86.68
7	Block 1	9	40	400	20	97.48
8	Block 1	5	15	200	40	77.82
9	Block 1	9	15	200	20	54.30
10	Block 1	7	27.5	300	30	67.71
11	Block 2	5	15	400	40	68.55
12	Block 2	9	15	200	40	65.71
13	Block 2	7	27.5	300	30	62.04
14	Block 2	5	40	200	40	79.73
15	Block 2	9	40	200	20	96.03
16	Block 2	9	40	400	40	94.29
17	Block 2	7	27.5	300	30	60.23
18	Block 2	5	15	200	20	67.41
19	Block 2	5	40	400	20	89.05
20	Block 2	9	15	400	20	53.94
21	Block 3	7	27.5	300	30	57.71
22	Block 3	7	27.5	300	30	57.12
23	Block 3	7	27.5	300	30	61.80
24	Block 3	7	27.5	100	30	52.43
25	Block 3	7	27.5	500	30	46.13
26	Block 3	7	27.5	300	50	82.67
27	Block 3	7	2.5	300	30	31.96
28	Block 3	11	27.5	300	30	64.50
29	Block 3	7	27.5	300	30	59.71
30	Block 3	7	27.5	300	30	60.80
31	Block 3	7	27.5	300	30	62.10
32	Block 3	3	27.5	300	30	66.90
33	Block 3	7	27.5	300	10	70.08
34	Block 3	7	27.5	300	30	62.04
35	Block 3	7	27.5	300	30	62.71
36	Block 3	7	52.5	300	30	82.13

Table 3. ANOVA of Response Surface Quadratic Model for Percentage Removal of Safranin

Source	Sum of squares	Degree of freedom	Mean square	F-Value	P-Value Prob > F	
Block	2469.27	2	1234.64			
Model	7017.89	14	501.28	22.78	<0.0001	Significant
A-pH	45.54	1	45.54	2.07	0.1666	
B-Contact time (min)	5104.17	1	5104.17	231.93	<0.0001	
C-Agitation speed (rpm)	168.33	1	168.33	7.65	0.0123	
D-Adsorbent dose (mg l^{-1})	145.83	1	145.83	6.63	0.0186	
AB	115.24	1	115.24	5.24	0.0337	
AC	69.72	1	69.72	3.17	0.0911	
AD	47.82	1	47.82	2.17	0.1568	
BC	20.43	1	20.43	0.93	0.3474	
BD	140.07	1	140.07	6.36	0.0207	
CD	10.96	1	10.96	0.50	0.4890	
A^2	187.06	1	187.06	8.50	0.0089	
B^2	73.59	1	73.59	3.34	0.0832	
C^2	85.16	1	85.16	3.87	0.0639	
D^2	816.16	1	816.16	37.09	<0.0001	
Residual	418.14	19	22.01			
Lack of fit	88.01	10	8.80	0.24	0.9819	Not significant
Pure error	330.12	9	36.68			
Core total	9905.30	35				
R-Squared			0.9538			
Adj R-squared			0.9123			
Pred R-squared			0.8894			
Adeq precision			21.599			
C.V.%			6.90			
Std. Dev.			4.69			
Mean			68.01			
Press			896.70			

Table 4. Freundlich and Langmuir Constants for Adsorption of Safranin on Biosorbent

Freundlich model			Langmuir model		
K_f (mg g^{-1})	n (l g^{-1})	R^2	q_m (mg g^{-1})	b (l mg^{-1})	R^2
1.483	2.014	0.9551	10.929	0.089	0.9924

Table 5. Kinetic Model Parameters for Adsorption of Safranin on Biosorbent

Pseudo-first order model			Pseudo-second order model		
q_e (mg g^{-1})	k_1 (min^{-1})	R^2	q_e (mg g^{-1})	K_2 (g mg^{-1} min^{-1})	R^2
5.799	0.023	0.9971	8.826	0.0109	0.9854

$$\log(q_e - q_t) = \log q_e - k_1 t/2.303 \quad (8)$$

Where q_e and q_t denote the amounts of dye adsorbed (mg g^{-1}) on biosorbent at equilibrium and at time t (min) respectively. These calculated K_1, q_e and correlation coefficient R^2 values are collected in Table 5.

Adsorption kinetic based on second order model is expressed by the following equation [32].

$$t/q_t = 1/k_2 q_e^{\ 2} + t/q_e \quad (9)$$

Where K_2 is rate constant of second order adsorption (g mg^{-1} min^{-1}), while k_2 is obtained from the intercept of plot t/q_t *vs*. t and q_e from slope.

RESULTS AND DISCUSSION

Characterization of Biosorbent

The knowledge of surface functional groups of a biosorbent material can give insight to the biosorption yield of the sorbent. FTIR spectroscopic analysis has played an important part in the investigation of biosorbent surface chemistry [33]. The FTIR spectrum of Phlomis cancellata Bunge shell is shown in Fig. 3. Several peaks were observed from the spectrum indicating that the prepared plant waste particles are composed of various functional groups which might be responsible for the dye biosorption. These groups will form active sites for biosorption of dye on the plant surface. The broad band at 3500 cm^{-1}, the peaks at 2919 and 2851 cm^{-1}, and the peaks at 1730 and 1633 cm^{-1} were attributed to the unbounded OH group, aliphatic CH group, and CO bond of carboxylic acid, respectively [34]. From the spectrum obtained, the peaks were observed in the region between 1000 and 1700 cm^{-1} can be assigned to hydroxyl and carbonyl groups and -C-O and –C-O-C stretching modes [35]. The peak at 1500 cm^{-1} may be due to the presence of aromatic rings [36]. The -COOH groups present on the surface of biosorbent can significantly bind the cationic dye safranin through the electrostatic interactions. Moreover, -OH groups can bind with the ammonium ion ($=N^+$) of the safranin molecule through the formation of hydrogen bonding interaction.

The analysis of SEM is useful for characterizing the surface morphology of biosorbent material (the particle

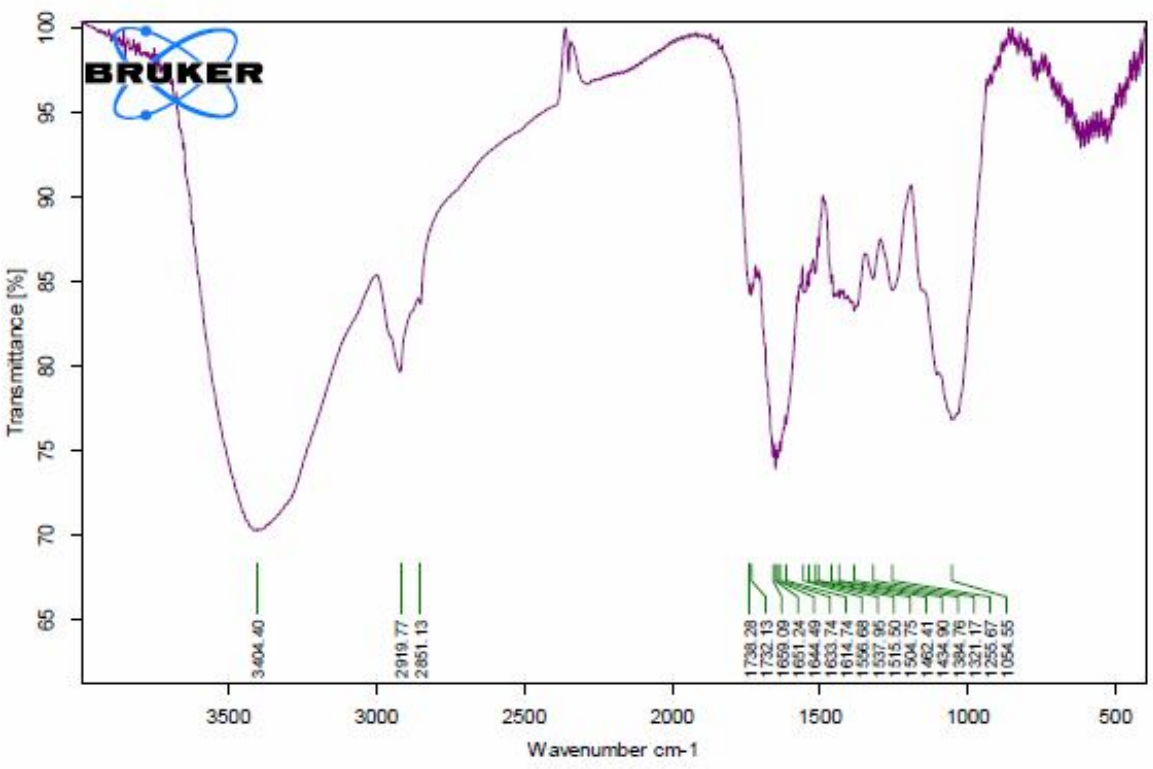

Fig. 3. FTIR spectrum of biosorbent.

shape, porosity, and appropriate size distribution of the biosorbent) and fundamental physical properties of the biosorbent surface. The SEM image of *Phlomis cancellata Bunge* is represented in Fig. 4. The figure shows irregular, rough, and porous surface morphology of the biosorbent material. The Phlomis Cancellata Bunge has considerable numbers of cavities and pores which indicates very high surface area and is a good possibility for the dye molecules to be trapped and biosorbed. Chemical analysis of the adsorbent by EDX showed that carbon, nitrogen and oxygen were the major constituents (Fig. 5 and Table 6). The C, O and N signals are attributed mainly to the polyphenol groups and other C, N, O-containing molecules in *Phlomis cancellata Bunge* leaf extracts. Specifically, the C, N and O is 47.63 wt%, 5.50 wt% and 46.87 wt%, respectively.

The zeta potential of biosorbent at different pH values were measured, and the results are shown in Fig. 6. It was found that the isoelectric point of sorbent was 7.4 and the surface of sorbent was negatively charged when pH higher than 7.4. The negatively charged surface could promote the adsorption capacity of cationic pollutants.

Statistical Analysis of Regression Model

In the present work, the effect of four factors, pH level, Contact Time, Agitation Speed and Adsorbent Dose, on the adsorption of safranin dye on the biosorbent obtained from leaves of Phlomis Cancellata Bunge was investigated. To find the most suitable fitting of the experimental data, a response surface model was developed using the regression analysis by considering different combinations of the linear, quadratic and interaction terms in polynomial equations which may be expressed as the following equation:

$$R_1 = +123.97557 - 12.75801 \times A + 0.31295 \times B - 3.49583E - 004 \times C - 1.32120 \times D + 0.10735 \times A \times B + 0.010437 \times A \times C - 0.086438 \times A \times D + 9.04000E - 004 \times B \times D - 8.27500E - 004 \times C \times D + 0.61279 \times A^2 + 9.83933E - 003 \times B^2 - 1.65385E - 004 \times C^2 + 0.051199 \times D^2 \quad (3)$$

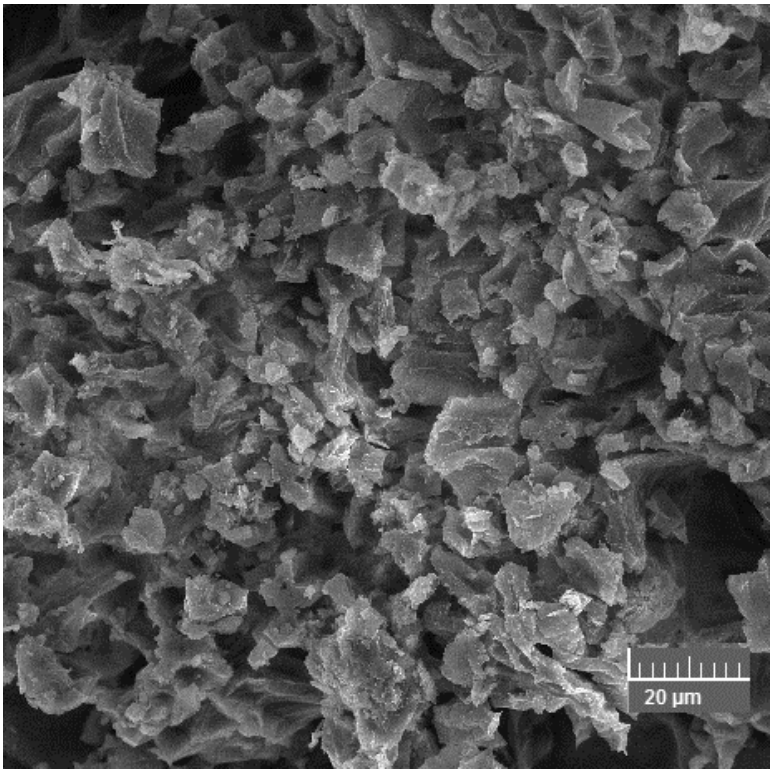

Fig. 4. SEM image of biosorbent.

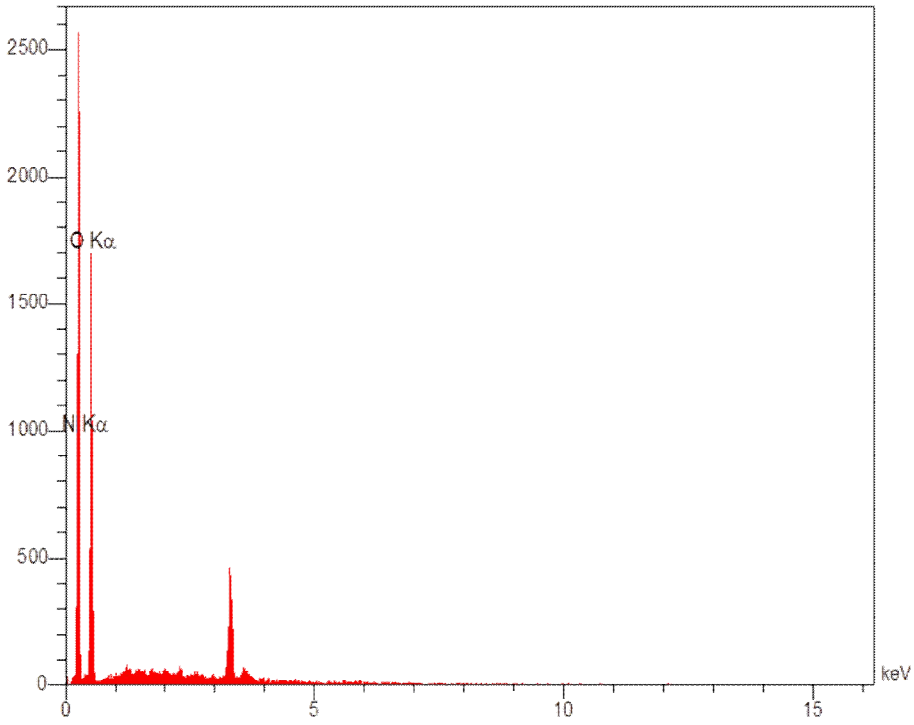

Fig. 5. EDX spectrum obtained for biosorbent.

Table 6. EDX Characterization Spectrum Obtained for Biosorbent

Elt	Int.	K	Weight%	Atomic%
C	590.8	0.7529	47.63	54.42
N	10.5	0.0166	5.50	5.38
O	427.3	0.2304	46.87	40.20
		1.0000	100.00	100.00

Figure 7a shows the normal probability plot of the residuals which reveals the systematic deviations from the expectations. The residuals are normally distributed if the points on the plot follow a straight line. The probability plot of the studentized residuals is to check for normality of residuals. As shown, all the internally studentized residual were randomly scattered across the graph and furthermore, there is no significant distribution pattern for all the diagnostics plots. The regression model resulted in a determination coefficient (R^2 = 0.9538) with a standard deviation of ±4.69, indicating that only 0.0462% of the variation can't be explained by the model. The adjusted determination coefficient at adjusted-R^2 = 0.9123, confirmed that the model was highly significant. As seen in Table 3, the prediction R-squared of 0.8994 was in acceptable agreement with the R-squared and showed a high predictive power of model. Adequate Precision measures the signal to noise ratio. A ratio greater than 4 is desirable. Our ratio of 21.599 favors the model since it is greater than 4. Table 3 presented F value and p-value of the variables included in the model. F value compares the mean square with the residual mean square. The model F-value implies the model is significant. P-value (Prob > F) is the probability of seeing the observed F value and a parameter to see if the null hypothesis is true (there are no factor effects). A P-value lower than 0.0001 was found, demonstrating again the high significance of the regression model. As seen, the F-value of lack of fit (LOF) of 0.24 indicated that the LOFs were not significant relative to the pure errors.

3D Response Surface Plot and Optimization

The three-dimensional reaction surface plots were constructed to achieve better understanding of the effects of independent variables and their interactions on the dependent variable. Interactions between the variables can also be clearly seen from the perturbation plot in Fig. 7b, which came up by default from the design expert software and perturbation theory using mathematical methods for finding an optimized condition to removal of safranin. Figures 8a-e showed 3D response surface plots for percentage removal of safranin on biosorbent as a function of pH level, contact time, agitation speed and adsorbent dose.

Figures 8a, d and e explains that by increasing the contact time from 15 min to 40 min , the removal of safranin increased to extent limit depending on the second tested variable. It may be attributed to more vacant active sites being available on the biosorbent surface for further dye biosorption until equilibrium. Figures 8a, b and c demonstrates that pH has a strong significance on removal of safranin and with the increase in pH value from 5 to 9, the adsorptivity increased and the maximum removal was achieved at pH 9. It is well known that the pH of the safranin solution influences the surface charge of the biosorbent, the dissociation of functional groups present on the biosorbent as well as the degree of ionization of the safranin. Below pH 7.4, the sorbent surface is positively charged due to protonation of surface functional groups sorbent, whereas above pH 7.4, sorbent will be positively charged related to dehydroxylation or deprotonation of the sorbent surface groups. As the pH decreased from 9 to 5, dye removal decreased which could be attributed to decreasing electrostatic attractions between the safranin and biosorbent molecules. Also, low biosorption of safranin at lower pH is due to the high concentration of H^+ ions which

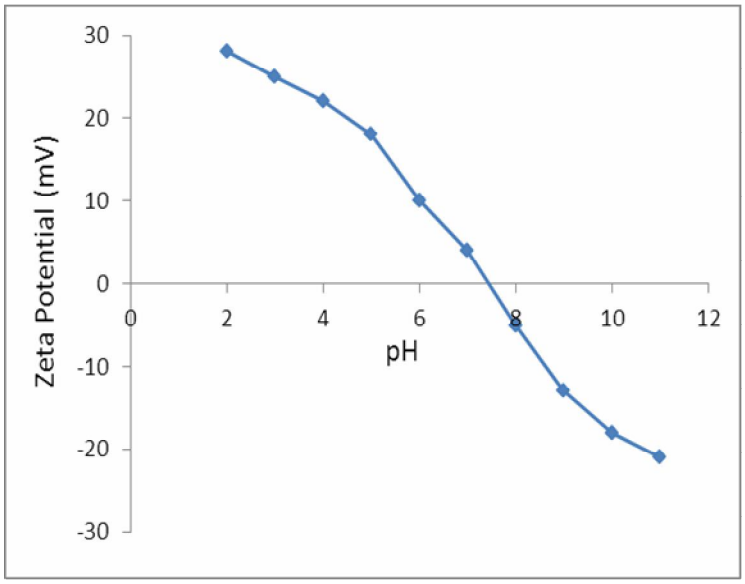

Fig. 6. Zeta potential of biosorbent *versus* pH.

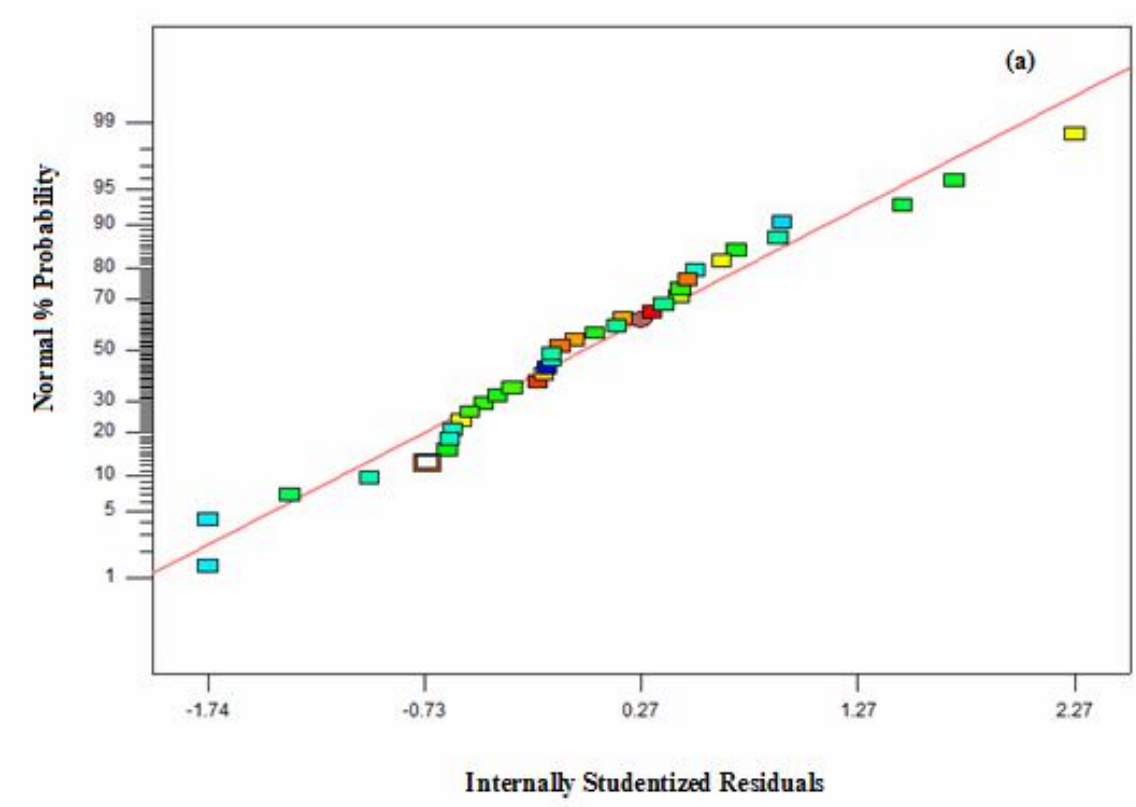

Fig. 7. Normal plot of residuals (Internally Studentized Residuals) (a), Perturbation plot of safranin dye removal (b), Residual *vs*. Run (Internally Studentized Residuals) (c)

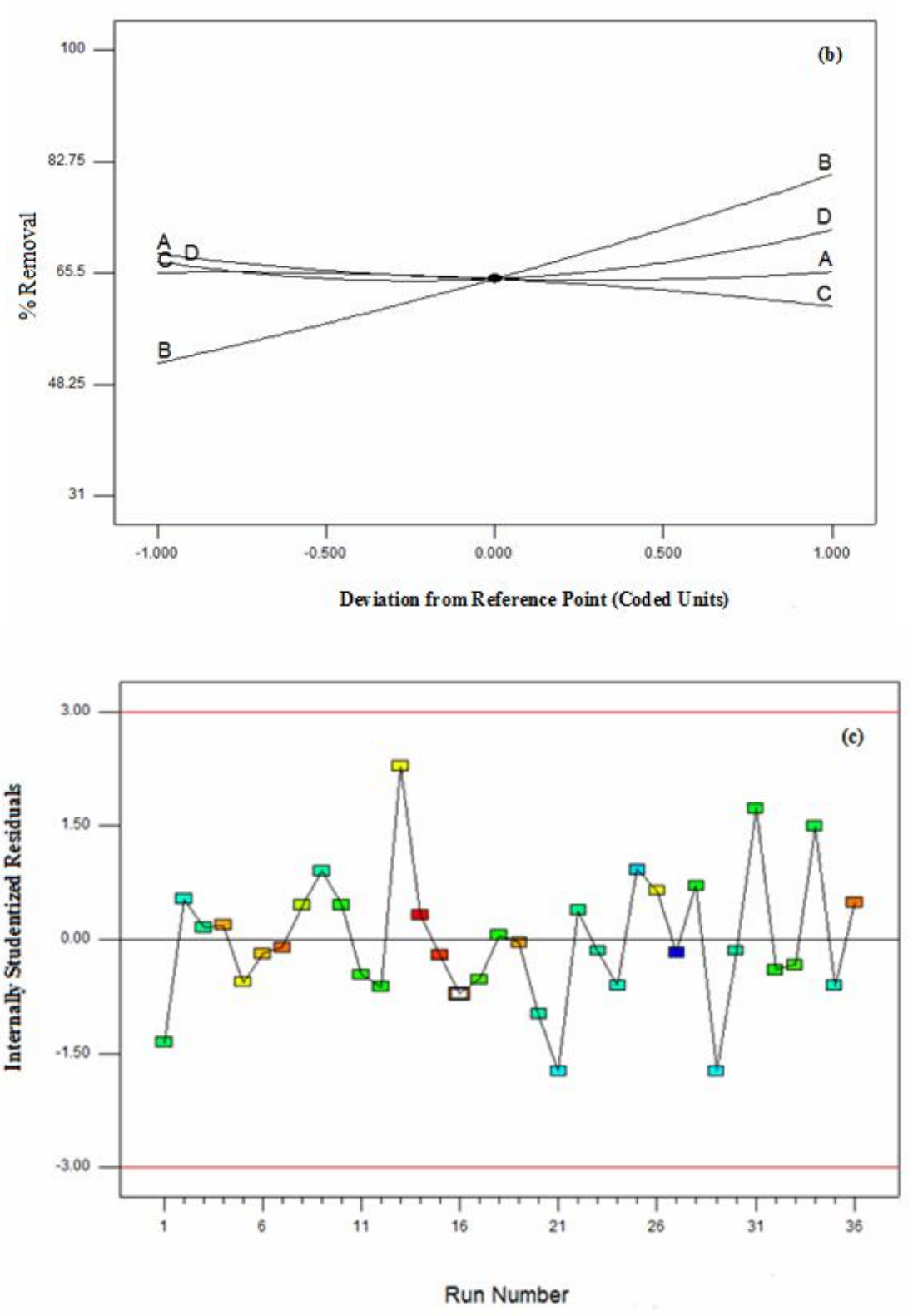

Fig. 7. Continued.

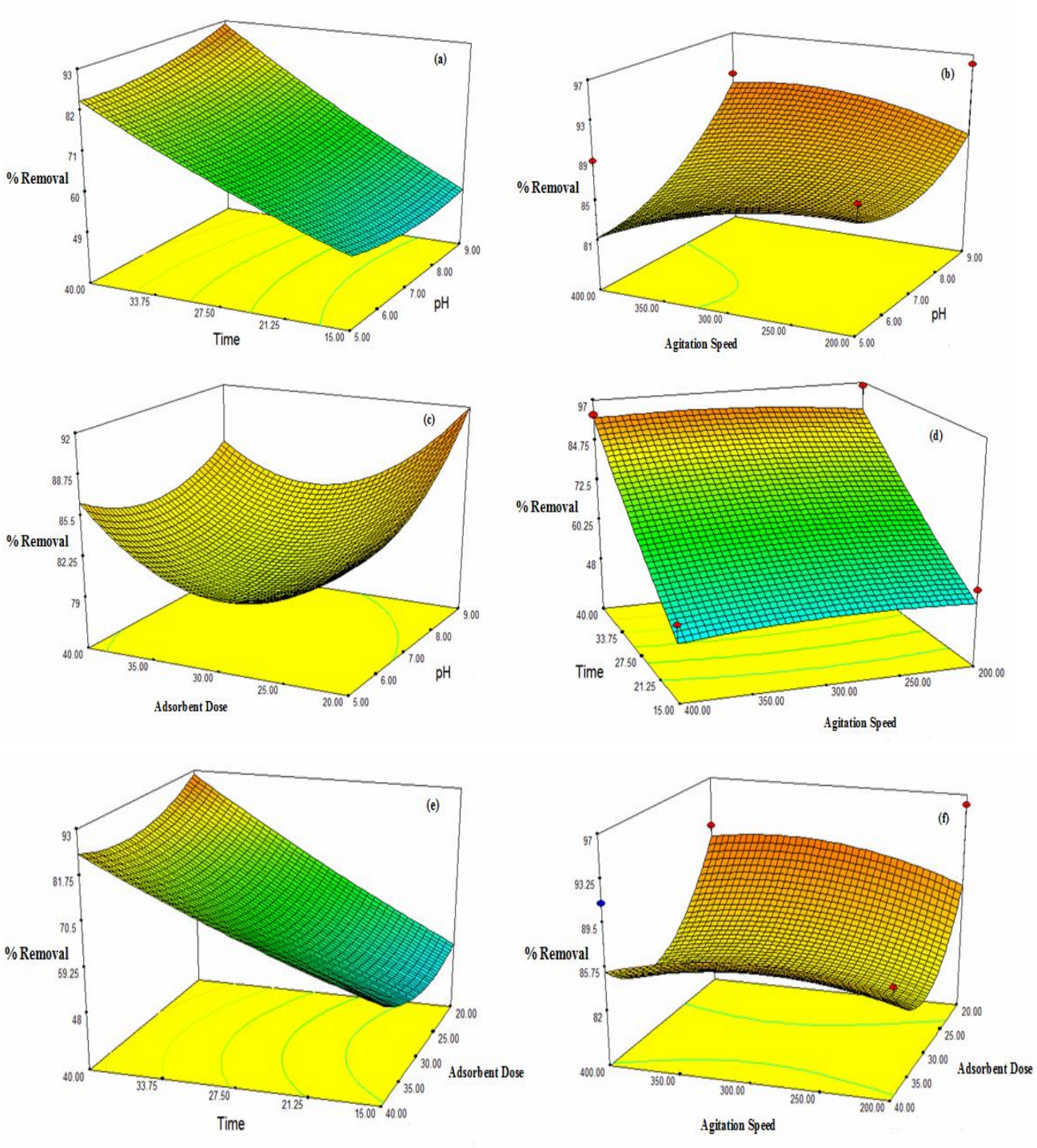

Fig. 8. Estimated response surfaces with related contours by plotting absorbance *versus* (a) pH (A) and Time of reaction (B); (b) agitation speed (C) and pH (A); (c) pH (A) and dosage of sorbent (D); (d) Time of reaction (B) and agitation speed (C); (e) Time of reaction (B) and dosage of sorbent (D); (f) agitation speed (C) and dosage of sorbent (D).

result in repulsion and hence cause the reduced biosorption at lower pH [37]. As the pH increases, more negatively charged surfaces are available resulting in decrease in repulsion between the positively charged dye molecule and the biosorbent.

Figures 8c, e and f show that sorbent dosage is one of the vital parameter to control the sorption efficiency in the study. The results demonstrate that on increasing the dose of biosorbent from 20 to 40 mg l^{-1}, the adsorptivity decreased. The reduced sorption capacity at higher sorbent dosage is attributed to the unsaturation of adsorption sites as aggregation might form between the sorbent, resulting in a decrease of external surface area and an increase of diffusional path length. Figures 8b, d and f showed that the removal of safranin increased with increase in agitation speed from 200 to 400 rpm and the maximum removal was achieved at agitation speed 331.18 rpm which is in agreement to previous findings with Congo red dye onto orange peel [38]. Some studies [39,40] revealed that variation of agitation has remarkable effect on the sorption capacity, as well as the rate of sorption process whereby boundary layer of the sorbent was minimised at high shaking rate.

The statistical and perturbation plot analysis suggest that the maximum optimized conditions for safranin dye (contact time 39.96 min, pH 9, agitation speed 331.18 rpm and adsorbent dose 20 mg l^{-1}) which showed 99.60% removal of dyes. In order to confirm the optimized experimental condition, four additional experiments were performed using the maximum predicted conditions and the average results are shown in Table 7. The results indicate a good agreement between the predicted and experimental response which demonstrate the high performance of the model.

Adsorption Kinetics and Isotherm Study

Langmuir and Freundlich isotherm models are applied to derive the adsorption parameters. 1/n, Freundlich constant value is less than 1 affirming favorability of the applied model. The best fit of the data is obtained using Langmuir isotherm model with a high R^2 value of 0.9924. Various parameters like q_m and K_L are calculated to be 10.93 mg g^{-1} and 0.0887 l mg^{-1}. The results depicted a monolayer adsorption rather than a multilayer adsorption process.

According to Dubinin-Radushkevich model, the mean free energy for adsorption of safranin by biosorbent is found to be 0.3 kJ mol^{-1}. This presents that predominant mechanism of the adsorption of dye by biosorbent is likely physical biosorption.

Adsorption kinetic based on pseudo-first-order model displays the linear plot with a correlation coefficient (R^2 = 0.9971). Therefore, pseudo-first-order kinetic model is appropriate for assessment of adsorption kinetic of dye on biosorbent surface.

Removal of Safranin from Real Samples Using Biosorbent

To evaluate the applicability of the proposed method, the removal of safranin from industrial wastewater and groundwater samples were performed. All the samples were spiked with safranin standard at 10 mg l^{-1}; subsequently, the removal process was studied by standard addition method. Dye removal, in all the samples, was more than 90% which reveals the effectiveness of this method for all samples.

CONCLUSIONS

The present work demonstrates that Phlomis cancellata Bunge has much potential as an inexpensive, abundant and easily available adsorbent for the removal of safranin from water samples. The impacts of pH, contact time, agitation rate and sorbent dosage on the removal of safranin was examined using response surface methodology and employing a central composite design Experimental. The significance of independent variables and their interactions were tested by analysis of variance. Under optimum conditions (contact time 39.96 min, pH 9.0, agitation speed 331.18 rpm and adsorbent dose 20 mg ml^{-1}), the maximum sorption capacity for safranin was found to be 99.60%. The kinetics of dye sorption fitted well with pseudo-first order kinetic model. The best fit of the data is obtained using Langmuir isotherm model with a high R^2 value of 0.9924. Various parameters like q_m and K_L are calculated to be 10.929 mg g^{-1} and 0.0887 l mg^{-1}. The mean free energy for adsorption of safranin by biosorbent is found to be 0.3 kJ mol^{-1}. This presents that predominant mechanism of the adsorption of dye by biosorbent is likely physical

Table 7. Predicted and Experimental Values of Response at Optimum Conditions

pH	Contact time (min)	Agitation speed (rpm)	Adsorbent dose (mg ml^{-1})	Response		Error
				Predicted (%)	Experimental (%)	
9	39.96	331.18	20	99.60	98.41	0.61

Table 8. Comparison of the Performance of the Present Biosorbent for Removal of Safranin with other Biosorbent

Adsorbent	Contact time (min)	Removal efficiency (%)	Ref.
Bambusa tulda	60	98.67	[41]
Nile rose plant	50	98.40	[42]
Pineapple peels	90	43.30	[43]
NaOH-treated rice husk	45	96.92	[44]
Phlomis cancellata bunge	39.96	99.60	This work

biosorption. The performance of biosorbent was comparable with other previously reported biosorbents for removal of safranin, as shown in Table 8. It can be seen that high percentage of safranin was removed from the sample by using Phlomis cancellata Bunge. Also, the time required for the removal of dye on the surface of biosorbent was less than that for other biosorbents.

ACKNOWLEDGEMENTS

The authors acknowledge the financial support of this work by University of Torbat-e jam, Torbat-e jam, Iran.

REFERENCES

[1] M. Zamouche, S. Arris, MB. LeHocine, Int. J. hydrogen. Energy 39 (2014) 1523.
[2] S.P. Shukla, A. Singh, L. Dwivedi, K.J. Sharma, D.S. Bhargava, R. Shukla, N.B. Singh, V.P. Yadav, Markandeya, Int. J. Sci. Innov. Res. 2 (2014) 58.
[3] V.K. Gupta, A. Mittal, R. Jain, M. Mathur, S. Sikarwar, J. Colloid. Interface. Sci. 303 (2006) 80.
[4] L. Rejniak, H. Piotrowska, Nature 209 (1966) 517.
[5] F.B.A. Rahman, M. Akter, Int. J. Waste. Resour 6 (2016) 1.
[6] V.P. Kasperchik, A.L. Yaskevich, A.V. Bil'dyukevich, Petrol. Chem. 52 (2012) 545.
[7] M. R.Sohrabi, A. Khavaran, S. Shariati, S. Shariati, Arab. J. Chem. 10 (2017) S3523.
[8] S. Wijannarong, S. Aroonsrimorakot, P. Thavipoke, C. Kumsopa, S. Sangjan, Apcbef. Procedia 5 (2013) 279.
[9] H. Zou, W. Ma, Y. Wang, Arch. Environ. Prot 41 (2015) 33.
[10] H. Zou, Y. Wang, W. Ma, X. Han, Asian. J. Chem. 27 (2015) 3350.
[11] M.F Abid, M.A Zablouk, A.M Abid-Alameer, Iran. J. Environ. Health. Sci. Eng. 9 (2012) 17.
[12] R. Saravanan, E. Sacari, F. Gracia, M. Mansoob Khan,

V. Kumar Gupta, J. Mol. Liq. 221 (2016) 1029.
[13] N. Mohammadi, H. Khani, V. Kumar Gupta, E. Amereh, Sh. Agarwal, J. Colloid. Interface. Sci. 362 (2011) 457.
[14] A. Afkhami, M. Saber-Tehrani, H. Bagheri, J. Hazard. Mater. 181 (2010) 836.
[15] S.T. Akar, Y.Y. Balk, O. Tuna, T. Akar, Carbohyd. Poly. 94 (2013) 400.
[16] S. Nawaz, H.N. Bhatti, T.H. Bokhari, S. Sadaf, Chem. Ecol. 30 (2014) 52.
[17] I. Khatod, Int. J. Chemtech. Res. 5 (2013) 572.
[18] F. Deniz, Sci. World. J. 2014 (2014) 1.
[19] C.-H. Lin, C.-H. Gung, J.-J. Sun, S.-Y. Suen, J. Membrane. Sci. 471 (2014) 285.
[20] S.-L. Chan, Y.P. Tan, A.H. Abdullah, S.-T. Ong, J. Taiwan. Inst. Chem. Eng. 61 (2016) 306.
[21] Sh. Hasani-Ranjbar, B. Larijani, M. Abdollahi, Arch. Med. Sci. 4 (2008) 285.
[22] W.C. Evans, T. Evan, S. Pharmacognosy, W.B. Saunders Company Ltd., London, 1996.
[23] K. Morteza-Semnani, K. Moshiri, M. Akbarzadeh, J. Essent. Oil Res. 18 (2006) 672.
[24] H. Akhlaghi, A. Motavalizadeh Kakhky, J. Essent. Oil Res. 13 (2010) 650.
[25] M. Deylamsalehi, M. Mahdavi, A. Motavalizadeh Kakhky, A.M. Akbarzadeh, J. Mahmudi, S.F. Mirahmadi, Z. Ebrahimi, F. Abedi, Teop. J. 16 (2013) 555.
[26] M. Polo, M. Llompart, C. Garcia-Jares, R. Cela, J. Chromatogr. A 1072 (2005) 63.
[27] V. Czitrom, Am. Stat. 53 (1999) 126.
[28] D.C. Montgomery, J.R. Stat. Soc., Ser. D 48 (1999) 159.
[29] M.A. Bezerra, R.E. Santelli, E.P. Oliveira, L.S. Villar, E.A. Escaleira, L.A. Escaleira, Talanta 76 (2008) 965.
[30] M.J. Ahmed, S.K. Theydan, Chem. Eng. J. 214 (2013) 310.
[31] S. Lagergren, K. Sven. Vetensk. Akad. Handl 24 (1898) 1.
[32] Y.S. Ho, G. McKay, Chem. Eng. J. 70 (1998) 115.
[33] G. Blazquez, M.A. Martın-Lara, E. Dionisio-Ruiz, G. Tenorio, M. Calero, J. Ind. Eng. Chem. 18 (2012) 1741.
[34] S. Dawood, T.K. Sen, Water. Res. 46 (2012) 1933.
[35] P. Li, Y.-J. Su, Y. Wang, B. Liu, L.-M. Sun, J. Hazard. Mater. 179 (2010) 43.
[36] F.A. Pavan, A.C. Mazzocato, Y. Gushikem, Bioresour. Technol. 99 (2008) 3162.
[37] R.M. Kulkarni, Z.G. Srinikethan, K.V. Shetty, J. Biochem. Technol. 3 (2014) 158.
[38] C. Namasivayam, N. Muniasamy, K. Gayatri, M. Rani, K. Ranganathan, Bioresour. Technol. 57(1996) 37.
[39] G.Z. Kyzas, Materials 5 (2012) 1826.
[40] F.A. Batzias, D.K. Sidiras, J. Hazard Mater. 149 (2007) 8.
[41] N. Laskar, U. Kumar, Mater. Sci. Eng. 225 (2017) 1.
[42] A.B. Mohammed, A.R. Omran, M.A. Baiee, J.M. Salman, Baghdad. Sci. J. 15 (2018) 26.
[43] M.A. Mohammed, A. Ibrahim, A. Shitu, Int. J. Environ. Monit. Anal. 2 (2014) 128.
[44] S. Chowdhury, R. Mishra, P. Kushwaha, P. Saha, Asia-Pac. J. Chem. Eng. 7 (2012) 236.